



HAL
open science

Frost flowers growing in the Arctic ocean-atmosphere-sea ice-snow interface: 1. Chemical composition

Thomas A. Douglas, Florent Domine, Manuel Barret, Cort Anastasio, Harry
J. Beine, Jan Bottenheim, Amanda Grannas, Stephan Houdier, Stoyka
Netcheva, Glenn Rowland, et al.

► To cite this version:

Thomas A. Douglas, Florent Domine, Manuel Barret, Cort Anastasio, Harry J. Beine, et al.. Frost flowers growing in the Arctic ocean-atmosphere-sea ice-snow interface: 1. Chemical composition. Journal of Geophysical Research: Atmospheres, 2012, 117, 58, p. 73-95. 10.1029/2011JD016460 . insu-03622106

HAL Id: insu-03622106

<https://insu.hal.science/insu-03622106>

Submitted on 28 Mar 2022

HAL is a multi-disciplinary open access archive for the deposit and dissemination of scientific research documents, whether they are published or not. The documents may come from teaching and research institutions in France or abroad, or from public or private research centers.

L'archive ouverte pluridisciplinaire **HAL**, est destinée au dépôt et à la diffusion de documents scientifiques de niveau recherche, publiés ou non, émanant des établissements d'enseignement et de recherche français ou étrangers, des laboratoires publics ou privés.

Copyright

Frost flowers growing in the Arctic ocean-atmosphere–sea ice–snow interface:

1. Chemical composition

Thomas A. Douglas,¹ Florent Domine,² Manuel Barret,² Cort Anastasio,³ Harry J. Beine,³ Jan Bottenheim,⁴ Amanda Grannas,⁵ Stephan Houdier,² Stoyka Natcheva,⁴ Glenn Rowland,⁵ Ralf Staebler,⁴ and Alexandra Steffen⁴

Received 23 June 2011; revised 5 December 2011; accepted 15 December 2011; published 9 February 2012.

[1] Frost flowers, intricate featherlike crystals that grow on refreezing sea ice leads, have been implicated in lower atmospheric chemical reactions. Few studies have presented chemical composition information for frost flowers over time and many of the chemical species commonly associated with Polar tropospheric reactions have never been reported for frost flowers. We undertook this study on the sea ice north of Barrow, Alaska to quantify the major ion, stable oxygen and hydrogen isotope, alkalinity, light absorbance by soluble species, organochlorine, and aldehyde composition of seawater, brine, and frost flowers. For many of these chemical species we present the first measurements from brine or frost flowers. Results show that major ion and alkalinity concentrations, stable isotope values, and major chromophore (NO_3^- and H_2O_2) concentrations are controlled by fractionation from seawater and brine. The presence of these chemical species in present and future sea ice scenarios is somewhat predictable. However, aldehydes, organochlorine compounds, light absorbing species, and mercury (part 2 of this research and Sherman et al. (2012)) are deposited to frost flowers through less predictable processes that probably involve the atmosphere as a source. The present and future concentrations of these constituents in frost flowers may not be easily incorporated into future sea ice or lower atmospheric chemistry scenarios. Thinning of Arctic sea ice will likely present more open sea ice leads where young ice, brine, and frost flowers form. How these changing ice conditions will affect the interactions between ice, brine, frost flowers and the lower atmosphere is unknown.

Citation: Douglas, T. A., et al. (2012), Frost flowers growing in the Arctic ocean-atmosphere–sea ice–snow interface: 1. Chemical composition, *J. Geophys. Res.*, 117, D00R09, doi:10.1029/2011JD016460.

1. Introduction

[2] Springtime photochemical reactions in Polar Regions have been the focus of numerous recent research efforts due to their role in lower tropospheric phenomena including ozone depletion events and mercury depletion events. These events are catalyzed by halogens, particularly bromine [Barrie et al., 1988], which reacts vigorously with ozone to

make BrO and depletes ozone concentrations in air to values near zero [Bottenheim and Chan, 2006]. Enhanced BrO concentrations also oxidize gaseous elemental mercury to reactive gaseous mercury [Schroeder et al., 1998; Foster et al., 2001; Steffen et al., 2007] which is readily deposited to snow and ice surfaces [Lindberg et al., 2002; Douglas et al., 2008]. BrO rich air masses are typically found above snow covered sea ice [Richter et al., 1998; Simpson et al., 2007a], leads and polynyas [Zeng et al., 2003; Jones et al., 2006], and nilas ice and frost flowers on refreezing leads [Rankin et al., 2002; Kaleschke et al., 2004; Jones et al., 2006]. Frost flowers, ubiquitous on the thin skins of ice (nilas) that grows over refreezing sea ice leads, are featherlike, delicate ice crystals that form over a period of hours to days. Frost flowers provide a link between the ocean, sea ice, and lower troposphere through their unique growth process and chemical composition [Domine et al., 2005; Alvarez-Aviles et al., 2008; Obbard et al., 2009]. They have been implicated as a potential source of halogens [Rankin et al., 2002; Jones et al., 2006; Kalnajs and Avallone, 2006] and

¹U.S. Army Cold Regions Research and Engineering Laboratory, Fort Wainwright, Alaska, USA.

²Laboratoire de Glaciologie et Géophysique de l'Environnement, CNRS-INSU and Université Joseph Fourier-Grenoble I, Saint-Martin d'Hères, France.

³Department of Land, Air, and Water Resources, University of California, Davis, California, USA.

⁴Air Quality Research Division, Environment Canada, Toronto, Ontario, Canada.

⁵Department of Chemistry, Villanova University, Villanova, Pennsylvania, USA.

depleted sulfate [Wolff *et al.*, 2003] in Antarctica. Kaleschke *et al.* [2004] suggested that satellite BrO measurements were associated with “potential frost flower” areas which were locations where modeling suggested the presence of frost flower rich sea ice. Simpson *et al.* [2007a] found a positive correlation between BrO and contact with first year sea ice and concluded that sea salts in snow and sea ice are a major bromine source to the lower atmosphere. Douglas *et al.* [2005] provided the first mercury measurements from frost flowers and reported values up to 920 ng/L which were up to nine times higher than nearby coastal snow and approach the maximum contaminant level for mercury in United States drinking water. These studies suggest frost flowers on newly frozen sea ice leads play an active role linking the sea ice surface and the lower atmosphere.

[3] Due to the dynamic nature of sea ice there are thousands of square kilometers of frost flower fields forming in the Arctic at any time during the Polar winter and spring and, as shown by Bowman and Deming [2010], autumn. Recent observations show a reduction in summer ice extent [Serreze *et al.*, 2007; Stroeve *et al.*, 2007; Comiso *et al.*, 2008], a decrease in ice thickness [Rothrock *et al.*, 2008; Giles *et al.*, 2008; Haas *et al.*, 2008; Kwok and Rothrock, 2009], and a shift from a primarily perennial ice pack to seasonal ice [Shepson *et al.*, 2003; Rigor and Wallace, 2004; Nghiem *et al.*, 2006; Maslanik *et al.*, 2007]. This should provide a more dynamic ice environment with more open leads and thus increased potential for frost flower growth. As a consequence, a better understanding of the chemical composition of frost flowers over time and their role in boundary layer atmospheric chemistry are warranted.

[4] We undertook this study to quantify the chemical composition of frost flowers growing north of Barrow, Alaska in March and April 2009. We measured major ion and alkalinity concentrations, bulk pH, stable oxygen and hydrogen isotope values, organochlorine compound concentrations, soluble light absorbers, and aldehyde concentrations from melted snow and ice samples, brine and seawater. Our samples include seawater, brine, wet frost flowers, dry frost flowers, and snow. The study was part of the Ocean-Atmosphere-Sea Ice-Snow (OASIS) 2009 field campaign focused on the atmospheric chemistry of ozone and mercury depletion events in the Arctic. For many of the chemical species we measured these are the first values reported from frost flowers.

[5] Frost flowers grow on the surface of young sea ice because its temperature is significantly warmer than that of the overlying air. A water vapor flux is established from the young ice surface to the atmosphere. At a given height above the ice surface, or even at the very surface, the air becomes supersaturated with water vapor because of this flux, and ice crystal condensation can occur [Style and Worster, 2009]. However, the sea ice surface is for the most part flooded by fractionated seawater (brine) that is transported upward through ice grain boundaries toward the ice surface by the thermomolecular pressure gradient [Martin *et al.*, 1996]. The brine has salinities 50–100 parts per thousand by weight, up to three times the salinity of Arctic Ocean seawater [Simpson *et al.*, 2007a]. Frost flowers grow on small ice nodules (<1 cm in diameter) that stick out of the brine and act as nucleation sites because they are solid and they are slightly colder than the brine surface. Brine can wick onto the frost

flower skeleton [Rankin *et al.*, 2002; Domine *et al.*, 2005; Alvarez-Aviles *et al.*, 2008]. However, the timing between growth and wicking appears variable, as significant crystal growth has been observed [Domine *et al.*, 2005] before wicking was initiated. Hereafter, we refer to brine covered frost flowers as “wet” frost flowers and we call frost flowers whose surface is not covered by brine “dry” frost flowers.

[6] With regards to their formation process, frost flowers are fundamentally different from surface hoar crystals, which can also condense on snow and ice surfaces and commonly form on the snow and ice surface near sea ice leads [Douglas *et al.*, 2008]. The differences between frost flowers and surface hoar have been detailed by Style and Worster [2009]. Surface hoar forms by the condensation of atmospheric water vapor onto a snow or ice surface that has been radiatively cooled, usually at night. Surface hoar thus forms from a downward vapor flux whereas frost flowers form in an upward vapor flux so their composition is expected to reflect that of the surface that supplied the vapor.

[7] As sea ice grows its surface cools and frost flower growth eventually stops. If the surface becomes colder than the overlying air, typically at night because of radiative cooling, surface hoar may form onto frost flowers thereby adding water (as ice) mass. A visual examination can usually differentiate surface hoar from diamond dust, clear sky precipitation that falls under cold (below -20°C) low turbulence conditions [Intrieri and Shupe, 2004]. Frost flowers grow much faster than surface hoar, as indicated by their dendritic or needle shape, indicative of a Mullins-Sekerka growth instability that can only occur at high growth rates [Mullins and Sekerka, 1963]. Surface hoar crystals grow more slowly than frost flowers and are never dendritic.

[8] Frost flowers can also gain water (as ice) mass by trapping drifting snow. Aged frost flower clusters can therefore have a complex morphology with contributions from frost flowers, surface hoar and drifting snow crystals of various shapes, although typically these are small rounded grains. These multiple snow and ice sources (i.e., of meltwater volume in terms of concentration in mass per volume of water) play a role in the chemical composition of aged frost flowers. Since analyte concentrations are typically measured as mass per volume of water the addition of water volume (or in this case of snow or condensate with a low analyte concentration) would be expected to dilute the concentration of a given analyte.

[9] The brine that wicks up frost flowers leads to elevated concentrations of major ions (including halogens) in the frost flowers immediately following their formation. Vapor phase condensation is incrementally added to the frost flower skeleton and, as a consequence, the ratio of water vapor to brine in the frost flowers increases with time [Alvarez-Aviles *et al.*, 2008]. The seawater, sea ice, brine, and nodules are not a requisite of frost flower growth because frost flowers are also found on freshwater ice [Domine *et al.*, 2005]. In the case of frost flowers on sea ice the nodules provide a potential nucleus and the brine provides water vapor for deposition.

[10] Over a period of hours the frost flower crystals nucleate horizontally outward to lengths up to 5 to 10 cm. Their morphologies range from needles to dendrites depending on the air temperature during their formation [Perovich and Richter-Menge, 1994]. Their crystals have a specific surface area of roughly $18\text{ m}^2/\text{kg}$ which is about five

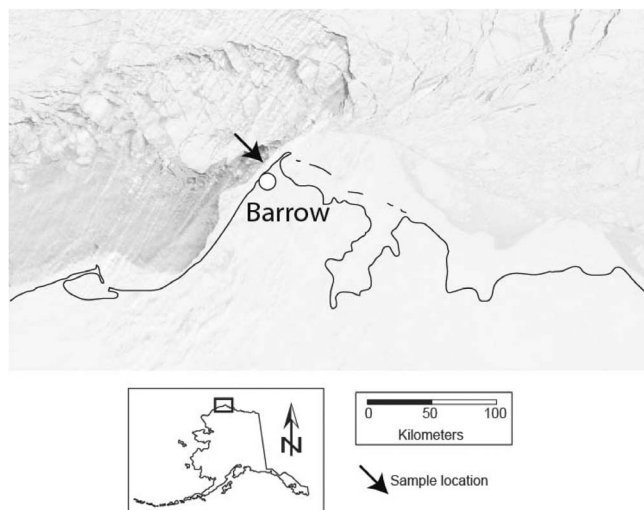


Figure 1. Moderate Resolution Imaging Spectroradiometer (MODIS) image of the Arctic Ocean Coast surrounding Barrow, Alaska on March 14, 2009, with a line drawing depicting the Arctic Ocean Coast and labels for the town of Barrow and the location where samples were collected between March 14 and March 25. Samples collected between March 31 and April 7 represent a variety of locations within 5 km of the March 14 to 25 location. Note the open water (grayish color) northwest of the sampling location.

times lower than freshly fallen snow [Domine *et al.*, 2005]. This low value is expected from their large size as specific surface area is inversely proportional to crystal size [Domine *et al.*, 2007]. Ultimately, frost flowers are covered with condensation (surface hoar crystals), entrained in winds [Wolff *et al.*, 2003], covered by snowfall or flooded with seawater.

2. Sampling and Analytical Procedures

2.1. Sample Collection Locations

[11] We traveled to multiple sites along the sea ice edge roughly five kilometers north of Barrow, Alaska in March and April, 2009. Frost flowers were collected from sites located at the edge of the boundary between the landfast ice and the open pack ice. Based on our previous experience at these locations, on the meteorology during this time, and on the analysis of Moderate Resolution Imaging Spectroradiometer (MODIS) imagery we believe the frost flowers we collected from March 14 to 25 were part of one large field that started to grow on March 13 or the morning of March 14 and remained growing in place for the following 10 days. MODIS images provide information on cloudy days (of which there were few during this period) and on the regional morphology and movement of sea ice during our field campaign. Figure 1 includes a MODIS image from March 14, 2009 and a location map for this study. A comparison of MODIS images from March 14 to 25 and global positioning system measurements taken at our sample sites during this period indicated we collected frost flowers from the same field from March 14 to 25. In addition, the frost flower fields we sampled were connected to the northern edge of the landfast ice region. As a consequence, though open water and floating ice passed by to the north of our

sampling locations to the north the frost flower fields we collected did not move during the study. From this analysis we believe the samples represent the continuum from wet, briny sea ice with initial frost flower growth (March 14) to further flower growth on an increasingly drying sea ice surface (March 16), to flowers increasingly being coated with vapor phase deposition (March 20 and 25; Figure 2).

[12] Additional opportunistic spot sampling from March 31 to April 7 included samples of frost flowers in various states of growth collected from a variety of locations. As such, they do not represent the continuum of growth stages represented in our March 14 to 25 samples. Air temperatures remained below -20°C between March 14 and April 8. Our field and laboratory research was carried out by multiple teams that traveled to the same field locations as a group. As a consequence, the ages and types of ice samples we collected and analyzed are identical. However, not every type of analysis was made from every sample collected and some teams did not collect samples on all of the days. So for some of the ice types we do not have results from the variety of measurements employed in this study.

2.2. Major Ion, pH, Alkalinity, and Oxygen and Hydrogen Stable Isotopes

[13] PTFE (Teflon) scoops were used to collect brine and frost flowers from the sea ice surface into high density polyethylene (HDPE) sample bottles. Care was taken to ensure that brine was not collected along with frost flowers. After the frost flowers were removed brine was collected from the ice surface. A 15 cm diameter hand augur was used to bore a hole through the ice to collect seawater samples. Samples were stored frozen and were thawed immediately prior to analysis.

[14] Samples for major ion analyses were filtered through acid washed $0.45\ \mu\text{m}$ polypropylene filters. Samples were diluted with $18\ \text{M}\Omega$ water 1,000 times (by volume) prior to analysis. All sample dilutions were done in quadruplicate (i.e., four separate diluted samples were created and analyzed per field sample) to assess cross sample variation in the dilution process. Results from the quadruplicate analyses suggest the dilutions are repeatable within 5% of the concentration values. Cation and anion concentrations were quantified on a Dionex ICS-3000 ion chromatograph with an AS-19 anion column and CS-12 cation column (Dionex Corporation Sunnyvale, California) at the Cold Regions Research and Engineering Laboratory Alaska Geochemistry Laboratory. Each sample had a 10 mL injection volume. A gradient method using potassium hydroxide eluent ranged from 20 mM to 35 mM for anion analyses. Cation analyses used methane sulfonic acid eluent with a concentration of 25 mM in isocratic mode. The system flow rate was 1 mL/min and the operating temperature was 30°C . The ion chromatograph was calibrated through repeat analysis of five calibration standards with concentrations ranging from 0.5 to 120 mg/L (within the range of analyses). Laboratory analytical anion and cation standards with values from 1 to 100 mg/L were analyzed repeatedly to verify system calibration and assess analytical precision. Based on these analyses the calculated precision for the analyses is $\pm 5\%$. Peaks were identified using Chromeleon (Dionex, Sunnyvale, California) and were verified visually.

[15] We measured carbonate alkalinity by Gran titration [Stumm and Morgan, 1996] from 40 mL of pure melted

March 14 6:30 pm



March 16 2:00 pm



March 20 1:00 pm



Figure 2. Photographs of the sea ice and frost flowers during the March 14, 16, and 20 sampling events. Photographs were not taken during the March 25 field work.

sample at 25°C. The initial bulk pH was noted for each sample and then 1 mL aliquots of 0.02 normal hydrochloric acid were added to the sample and the pH was measured following each acid addition. After roughly 10 acid additions the pH decreased to below 3 and the Gran function was calculated for each pH measurement. The x-intercept of a plot of the volume of acid added versus the Gran function was used to calculate the alkalinity. Repeat analyses of duplicate samples yielded an analytical precision of the alkalinity measurements of 10%.

[16] Stable isotopes of hydrogen and oxygen were measured using a Thermo Delta V mass spectrometer interfaced with a TC/EA pyrolysis oven (Thermo Scientific Waltham,

Massachusetts) at the University of Alaska Fairbanks Alaska Stable Isotope Facility. Samples were analyzed in triplicate. Multiple analyses of standards and replicate analyses of samples yielded a precision generally better than $\pm 0.4\%$ for oxygen ($\delta^{18}\text{O}$) and $\pm 2.0\%$ for hydrogen isotopes (δD). Data are reported in reference to VSMOW-SLAP-GISP calibration.

2.3. Organochlorine Compounds

[17] All of the samples for organochlorine analysis were collected on March 23. Seawater (30 kg) was obtained through a 20 cm diameter borehole through the ice. Frost flowers (24 kg) were sampled using a Teflon scoop and care

was taken to ensure the underlying brine layer was not collected. After the frost flowers were removed from the sea ice surface the underlying brine layer was collected (35 kg). All samples were placed into Teflon lined buckets that were sealed and returned to a laboratory at the Barrow Arctic Science Consortium (BASC).

[18] In the BASC laboratory sample buckets remained sealed and were allowed to melt until they reached 25°C. Melted samples were passed through glass columns containing fresh XAD resin (a proprietary solid phase extraction resin) that had been precleaned by accelerated solvent extraction (ASE; Dionex 2000, Sunnyvale, California) using a three-step mixed-solvent extraction sequence (100% acetone; 75%/25% acetone/hexane; 50%/50% acetone/hexane). The concentration of all analytes in the final cleaning extract was below the instrumental limit of detection for each analyte. After sample extraction was complete the XAD resin was transferred to a glass storage vial, spiked with 10 ng of 2,2',3,3',4,4'-hexachlorobiphenyl (PCB 128; Ultra Scientific, Kingston, RI, USA) as an internal recovery standard, and sealed for shipping back to the laboratory at Villanova University.

[19] Analytes were recovered from XAD by ASE using a 75%/25% hexane/acetone mix with magnesium sulfate added to the extraction cell for in situ drying of the sample; approximately 10 g of the extract was evaporated to a residual mass of approximately 0.1 g and the remainder was sealed for archiving. Determination of organochlorine pesticides and PCBs was carried out using a gas chromatograph (GC, Agilent 6890 N, Agilent Technologies, Palo Alto, CA, USA) fitted with a RTX-5 column (30 m length, 0.25 μm film thickness, Restek, Bellefonte, PA, USA) with mass spectrometric detection (Agilent 5973, Agilent Technologies, Foster City, CA, USA). One μL sample injections were made in pulsed splitless mode at an injector temperature of 250°C. The oven was initially held at 120°C for one minute, ramped at 4°C/minute to 250°C, ramped at 100°C/minute to 320°C then held for three minutes (run time: 37.2 min). The mass spectrometer was operated with negative chemical ionization using methane as the reagent gas and the detector in selected ion monitoring (SIM) mode. Two runs were performed for each sample; the first using a SIM program specific to pesticides and the second using a SIM program for PCBs. Quantitation of all analytes was performed using an external standard calibration using the ratio of analyte to internal standard to correct for variations in the extraction and MS ionization efficiency. Analytical curves were calculated from analyses of mixed calibration standards containing pesticides in hexane within the concentration range between 0.1 and 60 $\mu\text{g/L}$ for pesticides or 1 to 40 $\mu\text{g/L}$ for each of seven representative PCB congeners. The concentrations were scaled using the recovered internal standard to account for extraction efficiency, a sample blank correction was applied, and the average concentration of each analyte in the original environmental sample was calculated. Using external standards and a single internal standard compound means that the method should be regarded as semiquantitative only and the absolute concentration values may be unreliable. However, since the samples were processed and analyzed consecutively under identical conditions, results were subject to the same biases and are

indicative of the relative concentrations of the analytes in each sample type.

2.4. Soluble Light Absorbers

[20] Forty-five of the sea ice, brine, and frost flower samples that were collected between February 27 and April 15, 2009 were also analyzed for soluble light absorbers. Sample collection procedures (as outlined above) were optimized to ensure brine and frost flower samples were not contaminated with other sample materials. Samples were analyzed at a laboratory at BASC. The samples were stored at -20°C for up to three days prior to analysis. They were slowly melted in the laboratory to 25°C and analyzed for their UV-vis optical absorption using a 100-cm Liquid Wave Core Cell (LWCC) and a TIDAS spectrometer in the range between 220 and 600 nm. At 320 nm our $10\text{-}\sigma$ quantification level was on the order of $0.5 \times 10^{-3} \text{ m}^{-1}$. Our measured values were well above the $10\text{-}\sigma$ quantification level in the range up to 500 nm. More details of the sampling and analysis are described by *Beine et al.* [2011].

[21] Prior to absorption analysis we extracted two aliquots from each melted sample solution, froze them at -20°C , and shipped them to the laboratory in Davis, California where the aliquots were analyzed for H_2O_2 by High-Performance Liquid Chromatography (HPLC) and chloride was measured by ion chromatography. Laboratory protocols and results from additional analyses of snow samples are presented by *Beine et al.* [2011]. Nitrate and nitrite in sea ice, frost flower and brine samples were analyzed for NO_3^- by UV-vis absorption following quantitative reduction of nitrate to nitrite by V(III) in dilute acid and captured by Griess reagents to produce a red dye [*Doane and Horwath, 2003*]. This colorimetric method also yielded NO_2^- concentrations for the marine snow and ice samples, though the results likely underestimate the true NO_2^- concentration at the time the sample was collected because NO_2^- is not stable. The 3σ detection limits for H_2O_2 and NO_3^- were 75 nM and 2 nM, respectively.

[22] For each sample light absorption spectrum we subtracted the contributions from H_2O_2 and NO_3^- to determine the “residual absorption” ($\alpha_\lambda(\text{residual})$) at a given wavelength. As a consequence, the $\alpha_\lambda(\text{residual})$ spectra represent absorption due to “residual chromophores,” i.e., not H_2O_2 or NO_3^- . We then integrated the residual absorption spectra (e.g., between 300 and 450 nm to focus on photochemically active chromophores) to determine total absorption within that wavelength range ($\Sigma\alpha_\lambda(\text{residual})$). The residual part of the marine spectra is further analyzed for their content of colored dissolved organic carbon (CDOM) by H. J. Beine et al. (Soluble chromophores in marine snow, sea-water, sea-ice and frost flowers near Barrow, Alaska, submitted to *Journal of Geophysical Research*, 2012).

2.5. Aldehydes

[23] Snow, seawater, brine, and frost flower samples for aldehyde analysis were collected into 60 mL borosilicate glass vials with PTFE/silicone-lined caps (Kimble Glass Inc., Vineland, NJ). Sample collection procedures (as outlined above) were optimized to ensure that brine and frost flower samples were not contaminated with other sample materials. Vials were washed with ultrapure water and carefully rinsed before sampling. Vials were equilibrated to

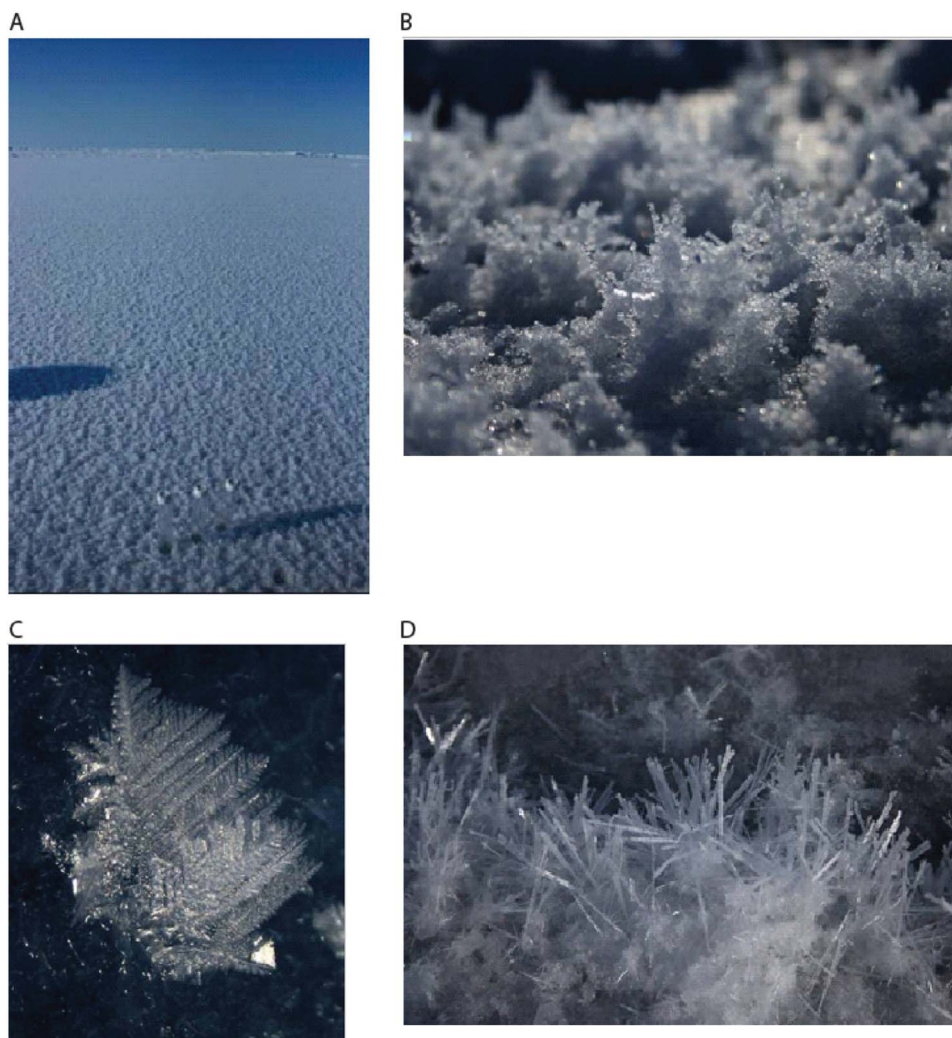


Figure 3. (a) Overview of the large frost flower field sampled on 2 April. (b) Close-up view of the frost flowers sampled on site 2 on 6 April. The height of the frost flowers is about 3 cm. (c) Close-up view of the frost flowers collected on site 3 on 6 April. Frost flower height: 1 cm. (d) Close-up view of frost flowers sampled on site 4 on 7 April. Frost flower height: 5 cm.

ambient temperature before sampling. Frost flowers were collected directly into the vials by carefully scraping the surface so samples entered through the vial's neck. Following collection, samples were stored at -40°C . On March 31 a 107 cm long ice core was extracted from first year ice. The sea ice was cored in two sections, yielding two cylinders 12 cm in diameter and 57 and 50 cm long. Ice cores were packed in polyethylene bags in the field and promptly transported to a -40°C cold room. Cores were subsequently sectioned using a stainless steel saw to obtain subsamples for chemical analysis. Lamellas of $90 \times 40 \times 10$ mm were obtained and immediately introduced in 100 mL Duran glass bottles (Schott, Mainz, Germany). In order to eliminate possible contamination introduced during the cutting procedure we removed the outer region of the ice core subsamples. Lamellas were thus kept to ambient temperature until about half the initial volume of ice melt. This initial meltwater was removed and the remaining ice was stored at -40°C until analysis.

[24] Frost flower samples for aldehyde concentration measurements were collected on March 23 and 25 and April 2. Between March 26 and March 31 winds moved the ice (and thus the frost flower field) to the west a few km and additional open water was exposed. Frost flowers growing on this open water were collected on April 2, 6, and 7. We differentiated 3 unique locations at the April 6–7 sampling location where frost flowers exhibited distinct morphologies (see Figures 3a–3d). Most of the time, leads opened during windstorms which allowed us to estimate the age of samples by assuming they started to form on young sea ice at the end of the storms. A total of 84 snow, brine and frost flower samples were collected during the campaign over sea ice. Triplicate samples were collected most of the time so we obtained 39 unique samples. We report here those samples that were collected in the frost flowers fields in coordination with the other chemical measurements.

[25] All samples were thawed at room temperature before chemical analysis by dansylacetamidooxyamine (DNSAOA) derivatization followed by HPLC separation

Table 1. Anion Concentration Mean and Standard Deviation Values From the Samples Collected Between March 14 and 25

Date	What	Number	Alkalinity ($\mu\text{M/L}$)		Chloride ($\mu\text{M/L}$)		Bromide ($\mu\text{M/L}$)		Sulfate ($\mu\text{M/L}$)		Σ^- ($\mu\text{eq/L}$)		Br/Cl Mean	SO ₄ /Na Mean
			Mean	Standard Deviation	Mean	Standard Deviation	Mean	Standard Deviation	Mean	Standard Deviation	Mean	Standard Deviation		
3/14/09	Wet frost flowers	4	3.4	1.4	2355.5	32.7	3.08	0.22	28.25	4.54	2418.3	34.8	0.001	0.016
3/14/09	Dry frost flowers	4	5.2	0.8	2259.3	208.4	2.80	0.27	26.28	2.62	2319.8	212.7	0.001	0.015
3/14/09	Brine	4	5.5	0.5	1705.0	71.8	2.25	0.42	58.18	9.02	1829.0	88.2	0.001	0.043
3/14/09	Surface snow	2	N/A	N/A	0.3	0.0	0.01	0.00	0.03	0.00	0.4	0.0	0.033	0.100
3/16/09	Dry frost flowers	4	2.1	0.5	1422.3	95.0	2.03	0.17	8.30	0.92	1442.8	95.9	0.001	0.009
3/20/09	Dry frost flowers	4	3.6	0.9	2040.5	187.8	2.65	0.58	49.48	7.46	2145.5	201.4	0.001	0.031
3/20/09	Seawater (8 cm thick ice)	2	1.6	0.1	569.5	96.9	0.70	0.00	27.90	5.23	627.5	106.8	0.001	0.059
3/20/09	Brine	4	2.6	1.1	1379.3	471.2	2.55	1.14	59.68	21.78	1504.0	507.4	0.002	0.053
3/20/09	Surface snow	2	N/A	N/A	0.6	0	0.02	0.00	0.01	0.00	0.6	0.0	0.033	0.025
3/25/09	10 day old frost flowers	2	2.1	0.0	304.0	1.4	0.35	0.07	1.40	0.00	309.0	1.4	0.001	0.007
	Seawater ^a				558		0.9		28.9		617		0.002	0.060

^aSeawater values from *Quinby-Hunt and Turekian* [1983].

and fluorescence detection as described by *Houdier et al.* [2000] with improvements detailed by *Houdier et al.* [2011]. Elevated salinity in samples was shown to reduce the reactivity of the DNSAOA reagent with the aldehydes studied here (M. Barret and S. Houdier, unpublished results, 2009). The salinity of each sample was thus measured by conductivity prior to analysis and most samples were diluted by an ad hoc factor to reduce salinity in the reacting solutions to no more than 10 practical salinity units (psu). The method is capable of measuring both linear aldehydes and dicarbonyls at the trace level. The limit of detection for reported aldehydes is in the 0.01–0.03 ppbw range. We only report here data for formaldehyde, acetaldehyde, glyoxal, and methylglyoxal. Traces of propionaldehyde and other uncharacterized carbonyls were also detected.

3. Results and Discussion

3.1. Major Ions, pH, Alkalinity, and Oxygen and Hydrogen Stable Isotopes

[26] Tables 1 and 2 include a summary of the major ion and alkalinity values measured from the frost flower, brine, sea ice, and seawater samples. Numerous samples of each sample type were collected and analyzed individually so the heterogeneity of the samples can be ascertained. Each

sample listed in Tables 1 and 3 represents the mean value measured from four individual diluted samples of that sample type. We present the mean and standard deviation values from two to four of these individual sample sets. During their initial growth the wet frost flowers exhibit the highest major ion and alkalinity concentrations and these values are roughly three times typical seawater. The alkalinity and major ion concentrations decrease over time such that the 10 day old flowers yielded major ion concentration values that are below seawater. For comparison, the seawater samples we collected on March 20 yield a chemical composition similar to the mean seawater values given by *Quinby-Hunt and Turekian* [1983]. Heterogeneity in concentration values over time is likely driven by vapor phase deposition to the frost flowers which will be discussed in detail below.

[27] There is no enhancement in bromide to chloride ratios in the frost flowers compared to brine or seawater (see bromide to chloride ratios for our samples in Table 1). However, all the frost flowers exhibit sulfate to sodium depletion compared to both seawater and brine (see sulfate to sodium ratios for our samples in Table 1). This is likely due to the precipitation of mirabilite at temperatures below -8°C [*Simpson et al.*, 2007b; *Morin et al.*, 2008]. The major ion concentrations and sulfate depletion we measured support previous measurements reported from frost flowers collected at Barrow [*Douglas et al.*, 2005; *Alvarez-Aviles et al.*, 2008]

Table 2. Cation Concentration Mean and Standard Deviation Values From the Samples Collected Between March 14 and 25

Date	What	Number	Sodium		Potassium		Magnesium		Calcium		Σ^+ ($\mu\text{eq/L}$) Mean
			Mean ($\mu\text{M/L}$)	Standard Deviation							
3/14/2009	Wet frost flowers	4	1780.5	38.5	42.5	1.3	241	6.9	38.5	1.3	2382.5
3/14/2009	Dry frost flowers	4	1719	150.3	39.8	3	223.5	13.3	32.8	3.3	2272
3/14/2009	Brine	4	1346.5	38	30	0	168.3	4.9	26.3	1.5	1763.8
3/14/2009	Surface snow	2	0.3	0	0	0	0	0	0	0	0.4
3/16/2009	Dry frost flowers	4	969.3	67.2	30	2.3	174.8	19.5	28.8	2.6	1406
3/20/2009	Dry frost flowers	4	1598.5	150.4	35.8	3.4	202.8	17.9	29.8	4.4	2099.3
3/20/2009	Seawater (8 cm thick ice)	2	473	80.6	10	1.4	59	9.9	11.5	0.7	309
3/20/2009	Brine	4	1125.8	378.1	24	8.3	137	46.7	21.8	6.7	1466.5
3/20/2009	Surface snow	2	0.4	0	0	0	0.1	0	0	0	0.6
3/25/2009	10 day old frost flowers	2	201.5	0.7	6	0	41.5	0.7	7.5	0.7	305.5

Table 3. The pH, Specific Conductance, Total Dissolved Solids, and Oxygen and Hydrogen Stable Isotope Mean and Standard Deviation Values From the Samples Collected Between March 14 and 25

Date	What	Number	pH		Specific Conductance ($\mu\text{S}/\text{cm}$)		Total Dissolved Solids (g/L)		$\delta^{18}\text{O}$ (‰)		δD (‰) Mean
			Mean	Standard Deviation	Mean	Standard Deviation	Mean	Standard Deviation	Mean	Standard Deviation	
3/14/2009	Wet frost flowers	4	7.43	0.14	168	4.3	84	2	-2.9	0.7	-22.3
3/14/2009	Dry frost flowers	4	7.97	0.1	169.1	2.9	84.8	1.1	-6.5	0.3	-49.3
3/14/2009	Brine	4	8.1	0.08	132.6	5.9	66.6	3.2	4.1	0.4	4.6
3/14/2009	Surface snow	2	N/A	N/A	N/A	N/A	N/A	N/A	-24.8	0.1	-172
3/16/2009	Dry frost flowers	4	7.92	0.03	120.2	4.9	60.1	2.5	-11.5	1	-77.5
3/20/2009	Dry frost flowers	4	8.02	0.14	123.9	18	61.9	8.5	-6.8	1.2	-56.4
3/20/2009	Seawater (8 cm thick ice)	2	8.26	0.4	47.6	4.3	23.8	2.2	-2.4	0.5	-23.7
3/20/2009	Brine	4	8.11	0.35	82.8	20.3	41.3	10	-0.5	0.4	-14.1
3/20/2009	Surface snow	2	N/A	N/A	N/A	N/A	N/A	N/A	-25.5	0.3	-177.3
3/25/2009	10 day old frost flowers	2	8.69	0.05	33.3	1.6	16	0.2	-18.1	0.1	-118.2
	Seawater ^a		7.43	0.14	168	4.3	84	2	-2.9	0.7	-22.3

^aSeawater values from *Quinby-Hunt and Turekian* [1983].

and Antarctica [*Rankin et al.*, 2002]. The frost flowers, surface snow, brine, and seawater samples all exhibit charge balance between the sum of cations (Na^+ , K^+ , Mg^{2+} , Ca^{2+}) and anions (alkalinity, Cl^- , Br^- , SO_4^{2-}).

[28] Alkalinity values have never been reported for frost flowers. The alkalinity concentrations we measured are slightly more heterogeneous than the values for the individual ions. This is likely not due to heterogeneous sample composition because the major ion values are more consistent among the samples of a given type. It is possible that the Gran titration technique we used, which has been commonly applied to surface waters, has limitations for these highly alkaline samples. Seawater generally has an alkalinity value of 2 to 2.5 mM/L while our seawater samples yielded values closer to 1.5 mM/L so our values can at least be seen as a close approximation of alkalinity. Our young, wet frost flowers yield alkalinity values of 3 to 5 mM/L, which are two to three times seawater and most of the major ions are enriched in the frost flowers at about this same amount. The alkalinity values of the frost flowers generally decrease with time, like the major ion concentrations, as frost flowers dry (i.e., are increasingly older).

[29] The bulk pH values we measured from seawater, brine, and melted frost flowers are all between 7.25 and 8.72 (Table 3). The young, wet frost flowers yield values around 7.4 and the pH appeared to increase slightly with age. The highest pH values were measured in the 10 day old frost flowers collected on March 25. Values previously reported for frost flower pH range from 8.1 to 8.7 [*Kalnajs and Avallone*, 2006]. Our values for dry, older flowers are within this range but our wet flowers are slightly less alkaline.

[30] Stable isotopes of oxygen and hydrogen have been used in numerous studies to determine moisture sources and the temperature of formation for wet and dry precipitation. We present the first oxygen and hydrogen stable isotope values of frost flowers and brine (Table 3 and Figure 4). Figure 4 includes a plot of the Meteoric Water Line (MWL) of *Craig* [1961] for reference. Surface snow in Barrow yields $\delta^{18}\text{O}$ values of $\sim -25\text{‰}$ that are what would be expected for precipitation condensing at -20°C [*Dansgaard*, 1964; *Jouzel and Merlivat*, 1984]. Vapor phase condensation of

surface hoar onto the frost flowers at -20°C would be expected to provide ice (water mass) with this value.

[31] On March 14 we collected brine, wet, and dry frost flowers and the brine yielded positive $\delta^{18}\text{O}$ values. The brine collected on March 20 had greater $\delta^{18}\text{O}$ values than seawater. This suggests the process that fractionates brine out of the sea ice crystal lattice also favors the fractionation of ^{18}O (and deuterium) over ^{16}O (and hydrogen). The smaller isotope likely fits into the ice crystal lattice slightly better than the larger isotope and, as a consequence, the brine has enriched stable isotope values. The March 14 and 20 brine samples are enriched in ^{18}O relative to deuterium when compared to the MWL.

[32] By comparing the March 14 and March 20 brine samples it is evident that the major ion concentrations of most analytes decreased over the one week time frame. The brine surface dried out over this same time (see photos in Figure 2) but the reasons for decreasing brine concentrations

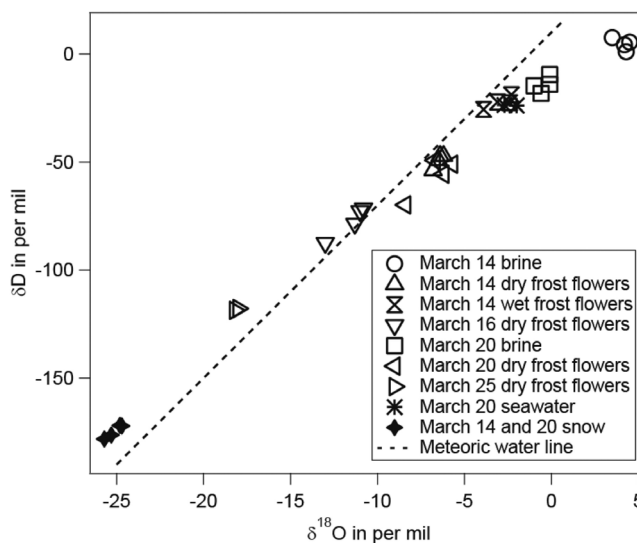


Figure 4. Stable hydrogen and oxygen isotope values measured from frost flowers, brine, surface snow, and seawater collected during this study.

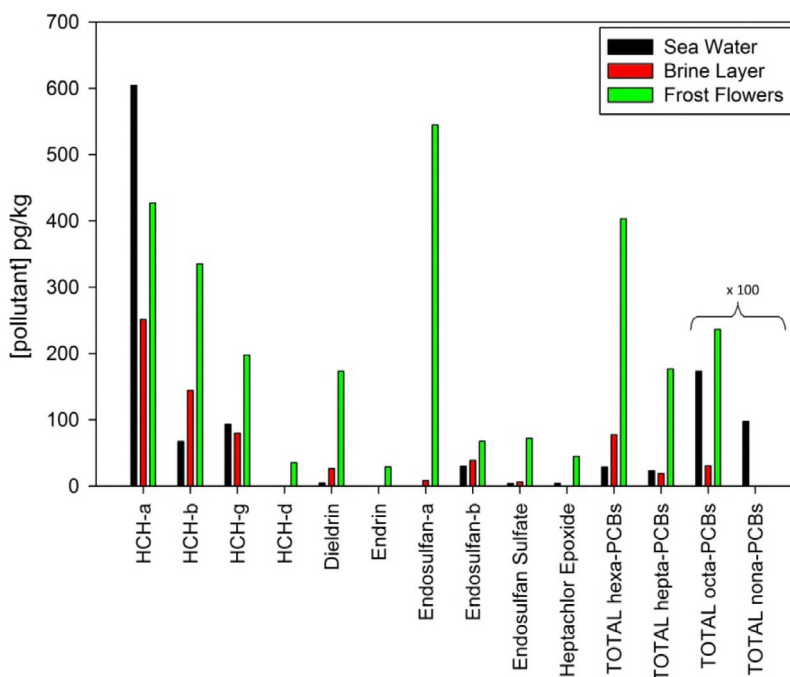


Figure 5. Measured concentrations (as pg per kg of melted sample) of organochlorine compounds (OCs) present in sea ice, brine, and frost flowers collected in March 2009 off the coast of Barrow, Alaska. Significant concentration enhancement in brine and frost flowers, relative to seawater, is observed for most OCs quantified via this method.

of major ions is not clear. Despite an overall decreasing trend in alkalinity and major ion concentrations from March 14 to March 25 the trend is not a simple or linear one. For example, there is some variation in the alkalinity and major ion concentrations from dry frost flowers collected between March 16 and 20 that could be attributable to sample heterogeneity or to a trend which we cannot discern with our data. However, overall, it appears the alkalinity, major ion and stable isotope values of the frost flowers change with time as the flowers incorporate more water mass (as ice) to their crystal skeleton.

[33] On both occasions for which we were able to collect brine and frost flowers growing from the brine (March 14 and 20) the frost flowers had roughly 7% lower $\delta^{18}\text{O}$ values than the brine. This is consistent with a fraction of the frost flower mass being formed by water vapor in equilibration with ambient temperatures of at least -20°C . The regions surrounding sea ice leads are highly moist [Andreas *et al.*, 2002; Douglas *et al.*, 2008] but our stable isotope results cannot be used to determine the condensate source(s). However, the most logical explanation of the stable isotope results is that the volume of the frost flowers comprised of vapor phase condensate increases with time because the frost flowers exhibit decreasing $\delta^{18}\text{O}$ and δD values as they age and dry. The 10 day old flowers yield $\delta^{18}\text{O}$ values of roughly -18‰ which suggests vapor phase precipitation at -20°C (i.e., a $\delta^{18}\text{O}$ value of -25‰) comprises a majority of the frost flower ice volume. Assuming an initial frost flower value of -2 to -5‰ roughly three quarters of the ice (water) mass at 11 days is attributable to condensation from the vapor phase. The fivefold decrease in major ion concentrations in

the old, dry frost flowers compared to the young, wet flowers is of a similar magnitude.

3.2. Organochlorine Compounds

[34] Organochlorine compounds (OCs) are an important class of anthropogenic pollutant that is transported to Polar Regions through a process known as global distillation [Arctic Monitoring and Assessment Programme (AMAP), 2009]. Because Arctic populations are at risk of bioaccumulation of these contaminants in the food web it is important to consider the physical transport pathways of these pollutants to and within the Arctic. Although a number of measurements of OCs in polar seawater and snow are reported in the literature [e.g., AMAP, 2009, and references therein], little work has been done to characterize organochlorine contaminants in sea ice [Lacorte *et al.*, 2009] and we know of no studies reporting OC concentrations in frost flowers or brine.

[35] Figure 5 shows the concentrations of OCs (blank corrected) measured in seawater, brine and frost flowers. In all cases but α -hexachlorocyclohexane (α -HCH) and nona-substituted PCBs the concentrations measured in frost flowers are highly enriched relative to the underlying seawater. It is known that salts are highly concentrated in frost flowers due to solute rejection, however this is the first evidence we are aware of that the same enrichment may also occur for hydrophobic organic compounds such as organochlorine contaminants and PCBs. Solute rejection can explain the seawater to brine concentration enhancement, but not the brine to frost flower enhancement, since, if anything, dilution by the mass of the ice skeleton would be expected. Two explanations can be proposed. First, OCs can

Table 4. Light Absorption Characteristics for the Samples Collected in This Study^a

Type	N	HOOH (μM)	Cl^- (mM)	NO_3^- (mM)	NO_2 (μM)	$\Sigma\alpha_\lambda(\text{Residual})$ (220–600 nm) (m^{-1})	$\Sigma\alpha_\lambda(\text{Residual})$ (300–450 nm) (m^{-1})
Marine surface snow	15	1.0 (± 1.5)	1860(± 2840)	3.6(± 2.2)		10.0(± 7.5)	1.3(± 0.7)
Seawater	3	0.6 (± 0.04)	569.3(± 68.6)	2.0(± 0.3)	2.5(± 1.5)	99.8(± 1.0)	19.8(± 0.3)
Sea ice	10	0.1 (± 0.04)		0.6(± 0.4)		22.3(± 5.3)	3.9(± 1.0)
Nilas	1	0.4	0.085	4		6.2	0.9
Brine	3	0.5(± 0.08)	1605(± 159.7)	20.3(± 10.6)	0.4(± 0.1)	136.5(± 26.5)	40.3(± 7.8)
Frost flowers	9	1.7(± 1.6)	1692(± 793.5)	21.6(± 7.6)	1.4(± 0.9)	189.1(± 23.7)	46.9(± 8.3)

^aShown are mean concentrations (except for nilas, which has only one sample) for HOOH, Cl^- , NO_3^- , and NO_2 , and the sum of residual absorption coefficients in the spectral ranges 220–600 nm and 300–450 nm. Values in parentheses are 1 standard deviation.

evaporate from the warmer brine and condensate onto the cold frost flowers. This would be another manifestation of the cryoconcentration effect of semi volatile organic compounds evidenced previously at much larger spatial scales [Blais *et al.*, 1998]. Alternatively, OCs from the atmosphere can dissolve into the brine that coats the frost flowers, because, however small, the solubility of OCs are much larger in liquids than in solid ice. Solubilization would be more rapid in the brine that coats frost flowers than in the brine at the ice surface or in seawater because of the large specific surface area of frost flowers [Domine *et al.*, 2005]. We expand on this issue when we discuss aldehydes below. However, it is difficult to make predictions based on our single sampling period.

3.3. Soluble Light Absorbers

[36] Table 4 shows the HOOH, chloride, nitrate, nitrite and amount of light absorption in the different types of samples we collected. Light absorption values are summed “residual” absorption coefficients, i.e., with the minor contributions from H_2O_2 and NO_3^- removed based on our snow sample results [Beine *et al.*, 2011]. The residual light absorption is due to humic-like substances (HULIS) or, perhaps, actual humic substances (D. Voisin *et al.*, Carbonaceous species and HUmic Like Substances (HULIS) in arctic snowpack during OASIS field campaign in Barrow, submitted to *Journal of Geophysical Research*, 2012) as well as unidentified chromophores. These values range from 6.2 to 194.7 and 0.9 to 49.3 m^{-1} for the spectral ranges of 220–600 and 300–450 nm, respectively (Table 4). For comparison, surface snow samples at Barrow show a mean $\Sigma\alpha_\lambda(\text{residual})$ of 9.8 ($\pm 49\%$) and 1.3 ($\pm 62\%$) (m^{-1}) in these respective ranges [Beine *et al.*, 2011, also submitted manuscript, 2012]. Thus the seawater, brine, sea ice, and frost flower samples have up to 38 times more light absorption in the solar range. Nilas, the first sea ice to form in calm waters, has approximately the same light absorption as snow.

[37] The chloride values presented in Table 4 represent means for the entire population of samples collected between February 27 and April 15. As such there is no easy way to compare the chloride concentrations presented in Tables 1 and 4. Despite this fact, except for the marine surface snow sample values in Table 4, the chloride concentrations in individual seawater, brine, and frost flower samples in Table 1 are within 20% of the concentration values given for populations of these same sample types in Table 4.

[38] The median NO_3^- concentration in Barrow snow was 3.7 μM [Beine *et al.*, 2011, also submitted manuscript,

2012]. Some of the frost flower samples had significantly greater NO_3^- concentrations, with maximum values up to 23.4 μM . In all samples, however, the contribution of the NO_3^- absorbance to the observed spectra was significant only below ca. 245 nm. H_2O_2 is only a minor contributor to the overall absorption in all samples.

[39] The results in Figure 6 show a strong correlation between the summed residual light absorption ($\Sigma\alpha_\lambda(\text{residual})$) and the Cl^- concentration in marine samples collected on March 20. This correlation suggests the chromophores are of marine origin and they accumulate from seawater to brine to frost flowers in a similar process as the major ions. This conclusion is consistent with that of Domine *et al.* [2011], who concluded that organic compounds in diamond dust were mostly of marine origin, and sourced from bubbles bursting at the surface and entraining organic compounds from the microlayer present at the surface of seawater in leads.

3.4. Aldehydes

[40] In addition to formaldehyde (HCHO, FA), the main aldehyde present in the atmosphere, α -dicarbonyls glyoxal (CHOCHO, GL) and methylglyoxal (CH_3COCHO , MG) have attracted particular attention over the past few years because of their potential role in secondary organic aerosol (SOA) formation [Ervens *et al.*, 2004; Carlton *et al.*, 2007; Fu *et al.*, 2008; Perri *et al.*, 2009]. In open oceans, the surface microlayer is photochemically active, producing

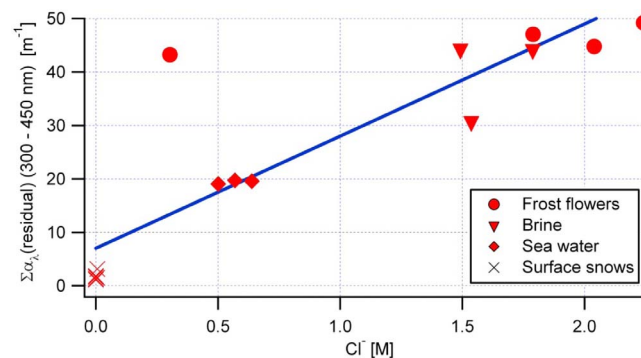


Figure 6. Relationship of residual absorbance ($\Sigma\alpha_\lambda$) in the 300–450 nm range versus Cl^- concentration for snow on sea-ice, seawater, brine and frost flower samples collected on March 20. The slope is 2.1×10^{-5} ($\pm 2.6 \times 10^{-6}$) ($\text{m}^{-1} / \mu\text{M Cl}^-$), (intercept 6.4 ± 3.2 , $R^2 = 0.817$, $N = 17$, $p = 0.0000$).

Table 5. Aldehyde Measurements From the Samples Collected During This Study

Date	Type	Age in Days ^a	Salinity (psu)	Formaldehyde (ppbw)	Acetaldehyde (ppbw)	Glyoxal (ppbw)	Methylglyoxal (ppbw)
23-Mar	Frost Flowers	na ^b	29.9	74.6	0.8	25.7	23.1
23-Mar	Snow	na	0.5	3.4	0.8	3.2	0.7
25-Mar	Frost Flowers	5	67.4	280.1	0.8	30.9	43.6
25-Mar	Brine	5	94.0	68.5	1.3	4.4	6.7
31-Mar	Ice Core	na	4.4	1.8	0.4	0.3	<LOD
2-Apr	Frost Flowers	2	120.0	39.9	10.1	20.2	15.3
2-Apr	Brine	2	57.1	8.3	4.6	2.1	2.8
2-Apr	Seawater	na	33.4	0.3	1.3	<LOD	<LOD
6-Apr	Frost Flowers	7	70.3	125.0	2.1	19.5	28.9
6-Apr	Frost Flowers	2	92.2	161.9	2.3	24.9	36.5
6-Apr	Frost Flowers	2	108.7	25.6	1.9	3.1	6.0
7-Apr	Frost Flowers	8	45.0	49.7	1.5	14.7	24.8
7-Apr	Brine	8	45.8	15.9	1.1	1.3	2.4
7-Apr	Frost Flowers	3	99.0	25.4	3.0	3.8	9.4
7-Apr	Brine	3	65.5	8.9	2.2	1.0	2.0
7-Apr	Frost Flowers	1	84.1	27.5	2.0	3.9	7.4

^aEstimated.^bNot available.

aldehydes [Zhou and Mopper, 1997] but also emits GL and MG precursors such as isoprene or terpenes [Shaw *et al.*, 2010]. Their mechanisms of production and exchanges between the surface of the sea and the atmosphere are not well understood [Sinreich *et al.*, 2010]. Interestingly, the lifetimes of GL and MG are limited to a few hours and these compounds can thus be considered as relevant indicators for oxidation reactions involving local precursors [Volkamer, 2005; Fu *et al.*, 2008; Huisman *et al.*, 2008; Stavrakou *et al.*, 2009]. Over sea ice, the atmosphere above open leads is highly convective [Alam and Curry, 1995], and we expect that, if marine precursors were present in the surface microlayer, they could efficiently be emitted to the atmosphere and subsequently scavenged by sea ice snow or frost flowers [Domine *et al.*, 2011].

[41] Aldehyde concentrations in the snow samples collected near frost flower fields were in the 1.5–3.5, LOD–0.8, 0.4–3.3, LOD–1.5 ppbw ranges for formaldehyde (FA), acetaldehyde (Ac), glyoxal (GL) and methylglyoxal (MG), respectively. These values are similar to those measured on the more intensively studied terrestrial snowpack [Domine *et al.*, 2011]. Frost flower samples exhibited systematically elevated concentrations for all aldehydes with the exception of Ac (Table 5). (FA) reached 280 ppbw for 5 day-old frost flowers, which is the highest value we measured for all types of samples collected. When analyzing brines near actively growing frost flowers, we found systematically lower concentrations for FA, GL and MG which were in the 8.8–74.9, 1.0–4.8 and 2.0–5.9 ppbw ranges, respectively. Very low aldehyde concentrations were observed in the seawater collected right under the fresh sea ice with only 0.3 ppbw of FA and undetectable amounts of GL and MG. Low levels were also found in the sea ice core in which aldehyde concentrations were almost homogeneous. The reported values for the ice core represents the mean value of the 10 subsamples analyzed.

[42] To our knowledge, the present results provide the first determination of carbonyl compounds in frost flowers. The total amount of aldehydes measured in brines and frost flowers is quite surprising and contrasts with the moderate to low levels measured in snow (collected on sea ice or land) or

sea ice. For comparison, the large concentrations measured in the 25 March frost flowers are of the same order of magnitude as those reported by Kawamura *et al.* [1996] in rain in Los Angeles. Anthropogenic emissions lead to elevated aldehyde concentrations in air [Sigsby *et al.*, 1987; Grosjean *et al.*, 2002; Corrêa *et al.*, 2010], and the strong concentrations we measured therefore raise questions as to their sources in frost flowers.

[43] Several hypotheses may explain the elevated aldehyde concentrations in frost flowers. First, because aldehydes are soluble in aqueous solutions, they could be scavenged from the atmosphere into the brine and then incorporated into frost flowers as they grow. The partitioning of aldehydes between the gas phase and brine is hard to determine because gas phase data for the aldehydes we measured have not been quantified over sea ice and the solubility of such compounds in highly saline solution is not well known. We propose here to test whether aldehyde concentrations can be explained by the presence of a liquid fraction in frost flowers, even though our calculations require approximations. As shown by Barret *et al.* [2011a], FA forms a solid solution with ice and it is possible to calculate the solubility of FA in ice and in water, knowing the partial pressure of FA, P_{FA} and the sample temperature. Assuming frost flowers can be considered as a mixture of ice and liquid water we can estimate the fraction of liquid water required to explain FA concentrations. By taking a mean $P_{FA} = 250$ pptv [Barret *et al.*, 2011b], a temperature of 243 K, and assuming that the solubility of FA in water can be extrapolated to negative temperatures in brines we calculate the solubility of FA in brine is 1300 ppbw while only 3.2 ppbw in ice. This indicates that a liquid fraction of 1 to 21% in frost flowers can account for the FA concentrations observed. Dicarbonyls GL and MG are much more soluble in water than FA by 1 or 2 orders of magnitude [Zhou and Mopper, 1990; Ip *et al.*, 2009] and this may explain why they are so abundant in frost flowers, although their mixing ratio in the atmosphere is probably very low. It should be noted that the presence of SO_4^{2-} , which is abundant in frost flowers, further increases the solubility of GL in solution [Ip *et al.*, 2009].

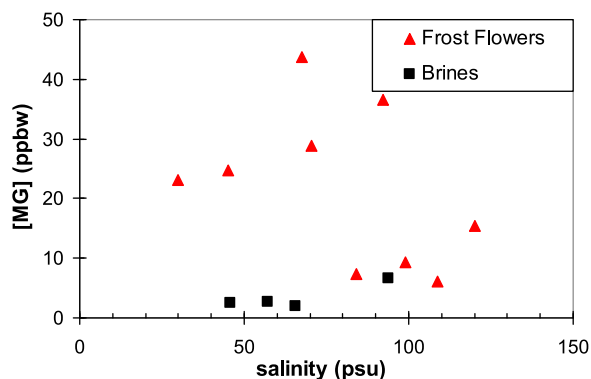


Figure 7. Methylglyoxal concentration as a function of salinity for frost flowers and brine samples.

[44] The effect of salinity on aldehydes was investigated because we expected this parameter could provide an indication of the liquid content of frost flowers. As shown in Figure 7 for MG, no correlation between salinity and aldehyde concentrations in frost flowers was found. This was also the case for the other aldehydes we measured.

[45] This lack of correlation is confirmed when we compare aldehyde concentrations in frost flowers and brine of the same age collected on the same day. Such analyses were performed on 25 March, 2 and 7 April. The salinity ratio frost flowers/brine ranges from 0.7 to 2.2, but the aldehydes are always more concentrated in frost flowers, with the exception of acetaldehyde on 25 March. The average enrichment between frost flowers and brine were 3.4, 1.7, 7.8 and 6.5 for FA, Ac, GL and MG, respectively.

[46] Since the liquid content of frost flowers is lower than that of brine the thermodynamic solubility of carbonyls in liquid water cannot fully explain why aldehydes are more concentrated in frost flowers than in brines. Kinetic aspects may be involved, as frost flowers have a large specific surface area and the brine layer on their surface is thin [Domine *et al.*, 2005]. Aldehydes could therefore be taken up by frost flowers much faster than by brine or seawater. This involvement of kinetics is consistent with the lower aldehyde concentrations we measured in seawater.

[47] Another possibility is that aldehydes are produced by organic precursors which were concentrated in frost flowers during their growth. When open leads start to freeze a brine layer forms at the surface of new ice and the substances dissolved are subsequently wicked up by frost flowers. Since the surface microlayer of oceans was shown to produce low molecular weight aldehydes [Zhou and Mopper, 1997], it appears possible that similar processes occur during frost flower formation. Although this marine production is not well understood [Sinreich *et al.*, 2010], it was proposed that photo-biochemical activity may be involved [Kieber and Mopper, 1987; Mopper and Kieber, 1991]. Bacteria exist throughout Polar Regions and can be active in media such as snow, impacting air-snow exchange [Amoroso *et al.*, 2010; Ariya *et al.*, 2011]. Since some bacterial strains can produce low weight carbonyls [Knietsch *et al.*, 2003] and because the bacterial and organic content of the brine [Møller *et al.*, 2011] from which frost flowers grow is large [Bowman and Deming, 2010], we speculate that photo-biochemical processes may occur in frost flowers and produce either the

aldehyde concentrations we measured or their organic precursors.

4. Conclusions: The Role of Frost Flowers in Lower Atmospheric Processes During Polar Spring

[48] Frost flowers occupy a key location between the lower atmosphere and the sea ice surface of Polar Regions. They are delicate, highly saline, and form repeatedly over thousands of square kilometers in the Arctic Ocean. It is expected that climate warming will lead to thinner ice that is more susceptible to dynamic processes that destroy ice and open leads. This scenario will lead to an expansion of the conditions that expose open water, create new ice, grow nilas, expose brine, and promote frost flower growth. As a consequence a better understanding of the chemical composition of frost flowers and their role in lower tropospheric atmospheric chemical processes is warranted.

[49] The bulk pH and alkalinity values we measured from brine and frost flowers have important ramifications on the role of the sea ice surface in lower atmospheric bromine chemistry. The heterogeneous reaction of HOBr with Cl^- and Br^- is largely controlled by pH with less efficiency as pH values become increasingly alkaline [Fickert *et al.*, 1999; Simpson *et al.*, 2007b; Morin *et al.*, 2008]. The pH of the snow and ice crystal surfaces relevant for heterogeneous atmospheric chemical reactions is not well known. Due to the alkaline composition of frost flowers (especially the older ones) they are unlikely to be a source of molecular bromine through the reaction of HOBr and Br ions. However, frost flowers may still be a source of gas-phase bromine [Kalnajs and Avallone, 2006] and they have been linked to BrO chemistry [Kaleschke *et al.*, 2004; Simpson *et al.*, 2007a, 2007b].

[50] Results from our major ion and stable isotope measurements support previous research that has shown frost flowers have both a briny, halogen rich component and a vapor phase component that is added over time [Douglas *et al.*, 2005; Alvarez-Aviles *et al.*, 2008]. This means the potential for frost flowers to promote heterogeneous chemical reactions in the lower atmosphere is greatest while they are initially forming from brine. The source of the vapor is likely the brine early during frost flower formation but over time, as the brine dries, the source is more likely condensation from vapor sourced from the locally high moisture environment.

[51] Frost flowers are also highly enriched in organochlorine compounds. Of the OCs we measured, most were present in frost flowers at far greater than the three to four-fold increase in major ions compared to seawater. Pućko *et al.* [2010a, 2010b] observed that HCH concentrations in snow over sea ice could increase by 50% due to the upward migration of brine from the sea ice surface, but they note the entrapment of brine and HCHs in ice depends on the rates of ice growth and on desalination. For the samples we collected there is no enrichment in α -HCH in the brine or frost flowers but there is an enhancement for the other HCH isomers and a number of organochlorines and PCBs.

[52] The α - and γ -HCH results are in general agreement with the work of Pućko *et al.* [2010a], who reported measurements of these two OCs in Canadian Arctic sea ice, lead ice and surface water. Although they do not report

measurements in frost flowers, their detailed study of the HCH isomers, combined with our “snapshot” of OC enrichment in sea ice brine and frost flowers, indicates that preferential solute rejection mechanisms from freezing seawater may need to be considered to adequately model POP fate and transport in frozen systems. The enrichment in OC between brine and frost flowers is indicative of a process unrelated to freezing, and which could be either fractionation caused by evaporation and condensation onto the colder frost flower surfaces or rapid dissolution from the atmosphere into the brine that coats the frost flowers, and which has a high specific surface area likely to enhance the rate of this process. With the data available, we cannot quantify the role of each process and we encourage caution in the interpretation of our single sample collection period. However, these initial data indicate that frost flowers may be an important consideration in OC cycling.

[53] We found a strong correlation between summed residual light absorption and chloride concentrations. This correlation suggests the chromophores are of marine origin and they likely accumulate from seawater to brine to frost flowers through a similar fractionation process that occurs for major ions. The frost flower samples yielded the highest residual light absorption values of any samples we collected. However, since the samples for these analyses were only collected once, we do not have the information on whether residual light absorption values are different in wet versus dry frost flowers or whether the concentrations or signatures changed over time.

[54] Frost flower aldehyde concentrations were generally greater than seawater, snow or brine samples and they do not exhibit any correlation with salinity. This supports our suggestion that their concentration is related to the liquid nature of the frost flower surface rather than to their salinity. The aldehydes could be scavenged from the atmosphere into the brine and/or the frost flowers. Our calculations suggest a liquid fraction of 1 to 21% in frost flowers can account for the elevated FA concentrations we measured. The increased solubilities of dicarbonyls GL and MG in water over FA may explain why these dicarbonyls are so abundant in frost flowers. The elevated SO_4^{2-} in frost flowers likely increases the solubility of GL in solution [Ip *et al.*, 2009]. The lack of a correlation between salinity and aldehyde concentrations in the frost flowers means the decrease in major ion concentrations and salinity, likely due to vapor phase deposition to the frost flowers, does not affect the aldehyde content. Another potential source of the aldehyde enrichment in frost flowers is that they were produced by organic precursors while they grew. It is possible that photo-biochemical processes occur in frost flowers and produce either the aldehydes we measured or their organic precursors.

[55] In summary, major ion concentrations, stable isotope values, and chromophore concentrations appear to be controlled by fractionation out of the ice lattice and the subsequent deposition of vapor phase condensate (from brine or the lower atmosphere). As a consequence, these chemical species exhibit decreasing concentrations as the brine dries and the frost flowers are increasingly coated by condensate. Knowledge of ice conditions, the age of the frost flowers and the local meteorology could be used to model the presence of these chemical species in the sea ice environment now

and in future scenarios with a changing sea ice and brine surface regime.

[56] However, aldehydes, organochlorine compounds and mercury concentrations [Douglas *et al.*, 2005; Sherman *et al.*, 2012] appear to be deposited to frost flowers through potentially unique processes that are not as well understood or predictable. These processes are likely related to both the fractionation of compounds during ice and brine formation and to chemical processes that occur on the halogen rich frost flower and brine surfaces. As a consequence, the present and future expected concentrations of these constituents in frost flowers may not be easily predicted.

[57] **Acknowledgments.** This work is part of the international multi-disciplinary Ocean-atmosphere-Sea Ice-Snowpack (OASIS) program. The numerous collaborators, science teams, and researchers from the OASIS campaign are gratefully acknowledged. Douglas’ research was supported by the U.S. National Science Foundation, the National Aeronautic and Space Administration, and the U.S. Army Cold Regions Research and Engineering Laboratory. F. Domine, M. Barret, and S. Houdier were supported by the French Polar Institute through grant IPEV 1017. They acknowledge Bruno Dellile, Nicolas-Xavier Geilfus and Gauthier Carnat from University of Liege for making it possible to collect ice core samples and Hans-Werner Jacobi for planning some of the sea ice sampling trips. H. Beine and C. Anastasio acknowledge the U.S. National Science Foundation Atmospheric Sciences ATM-0807702 and Tad Doane (UC Davis, LAWR) for the nitrate/nitrite analyses. A. Grannas acknowledges the U.S. National Science Foundation Grant ATM-0547435. Spencer Brown granted use of his photos from the March 20 sampling event. Don Perovich and Matthew Sturm provided insight into sea ice and snow in the Barrow area. Paul Shepson is acknowledged for providing insight throughout the field campaign. Son Nghiem provided information on the MODIS imagery. SnowNET data were provided by Matthew Sturm and colleagues. Discussions with Rolf Sander helped clarify our interpretation of the alkalinity measurements and results. The Barrow Arctic Science Consortium and Polar Field Services provided logistical support.

References

- Alam, A., and J. Curry (1995), Lead-induced atmospheric circulations, *J. Geophys. Res.*, *100*(C3), 4643–4651, doi:10.1029/94JC02562.
- Alvarez-Aviles, L., W. R. Simpson, T. A. Douglas, M. Sturm, D. K. Perovich, and F. Domine (2008), Frost flower chemical composition during growth and its implications for aerosol production and bromine activation, *J. Geophys. Res.*, *113*, D21304, doi:10.1029/2008JD010277.
- Amoroso, A., et al. (2010), Microorganisms in dry polar snow are involved in the exchanges of reactive nitrogen species with the atmosphere, *Environ. Sci. Technol.*, *44*(2), 714–719, doi:10.1021/es9027309.
- Andreas, E. L., P. S. Guest, P. O. G. Persson, C. W. Fairall, T. W. Horst, R. E. Moritz, and S. R. Semmer (2002), Near-surface water vapor over polar sea ice is always near ice saturation, *J. Geophys. Res.*, *107*(C10), 8033, doi:10.1029/2000JC000411.
- Arctic Monitoring and Assessment Programme (AMAP) (2009), *Arctic Pollution 2009*, 83 pp., AMAP, Oslo.
- Ariya, P. A., et al. (2011), Snow—A photobiochemical exchange platform for volatile and semi-volatile organic compounds with the atmosphere, *Environ. Chem.*, *8*(1), 62–73, doi:10.1071/EN10056.
- Barret, M., S. Houdier, and F. Domine (2011a), Thermodynamics of the formaldehyde–water and formaldehyde–ice systems for atmospheric applications, *J. Phys. Chem. A*, *115*(3), 307–317, doi:10.1021/jp108907u.
- Barret, M., F. Domine, S. Houdier, J.-C. Gallet, P. Weibring, J. Walega, A. Fried, and D. Richter (2011b), Formaldehyde in the Alaskan Arctic snowpack: Partitioning and physical processes involved in air-snow exchanges, *J. Geophys. Res.*, *116*, D00R03, doi:10.1029/2011JD016038.
- Barrie, L. A., J. W. Bottenheim, R. C. Schnell, P. J. Crutzen, and R. A. Rasmussen (1988), Ozone destruction and photochemical reactions at polar sunrise in the lower Arctic atmosphere, *Nature*, *334*, 138–141, doi:10.1038/334138a0.
- Beine, H. J., C. Anastasio, G. Esposito, K. Patten, E. Wilkening, F. Domine, D. Voisin, M. Barret, S. Houdier, and S. Hall (2011), Soluble, Light-Absorbing Species in Snow at Barrow, Alaska, *J. Geophys. Res.*, *116*, D00R05, doi:10.1029/2011JD016181.
- Blais, J. M., D. W. Schindler, D. C. G. Muir, L. E. Kimpe, D. B. Donald, and B. Rosenberg (1998), Accumulation of persistent organochlorine compounds in mountains of western Canada, *Nature*, *395*, 585–588, doi:10.1038/26944.

- Bottenheim, J. W., and E. Chan (2006), A trajectory study into the origin of spring time Arctic boundary layer ozone depletion, *J. Geophys. Res.*, *111*, D19301, doi:10.1029/2006JD007055.
- Bowman, J. S., and J. W. Deming (2010), Elevated bacterial abundance and exopolymers in saline frost flowers and implications for atmospheric chemistry and microbial dispersal, *Geophys. Res. Lett.*, *37*, L13501, doi:10.1029/2010GL043020.
- Carlton, A. G., B. J. Turpin, K. E. Altieri, S. Seitzinger, A. Reff, H. J. Lim, and B. Ervens (2007), Atmospheric oxalic acid and SOA production from glyoxal: Results of aqueous photooxidation experiments, *Atmos. Environ.*, *41*(35), 7588–7602, doi:10.1016/j.atmosenv.2007.05.035.
- Comiso, J. C., C. L. Parkinson, R. Gersten, and L. Stock (2008), Accelerated decline in the Arctic sea ice cover, *Geophys. Res. Lett.*, *35*, L01703, doi:10.1029/2007GL031972.
- Corrêa, S. M., G. Arbillia, E. M. Martins, S. L. Quitério, C. de Souza Guimarães, and L. V. Gatti (2010), Five years of formaldehyde and acetaldehyde monitoring in the Rio de Janeiro downtown area Brazil, *Atmos. Environ.*, *44*(19), 2302–2308, doi:10.1016/j.atmosenv.2010.03.043.
- Craig, H. (1961), Isotopic variations in meteoric waters, *Science*, *133*, 1702–1703, doi:10.1126/science.133.3465.1702.
- Dansgaard, W. (1964), Stable isotopes in precipitation, *Tellus*, *16*, 436–468, doi:10.1111/j.2153-3490.1964.tb00181.x.
- Doane, T. A., and W. R. Horwath (2003), Spectrophotometric determination of nitrate with a single reagent, *Anal. Lett.*, *36*(12), 2713–2722, doi:10.1081/AL-120024647.
- Domine, F., A. S. Taillandier, W. R. Simpson, and K. Severin (2005), Specific surface area, density and microstructure of frost flowers, *Geophys. Res. Lett.*, *32*, L13502, doi:10.1029/2005GL023245.
- Domine, F., A. S. Taillandier, and W. R. Simpson (2007), A parameterization of the specific surface area of seasonal snow for field use and for models of snowpack evolution, *J. Geophys. Res.*, *112*, F02031, doi:10.1029/2006JF000512.
- Domine, F., J. C. Gallet, M. Barret, S. Houdier, D. Voisin, T. Douglas, J. D. Blum, H. Balle, and C. Anastasio (2011), The specific surface area and chemical composition of diamond dust near Barrow, Alaska, *J. Geophys. Res.*, *116*, D00R06, doi:10.1029/2011JD016162.
- Douglas, T., M. Sturm, W. Simpson, S. Brooks, S. Lindberg, and D. Perovich (2005), Elevated mercury measured in snow and frost flowers near Arctic sea ice leads, *Geophys. Res. Lett.*, *32*, L04502, doi:10.1029/2004GL022132.
- Douglas, T. A., M. Sturm, W. R. Simpson, J. D. Blum, L. Alvarez-Aviles, G. Keeler, D. Perovich, A. Biswas, and K. Johnson (2008), The influence of snow and ice crystal formation and accumulation on mercury deposition to the Arctic, *Environ. Sci. Technol.*, *42*(5), 1542–1551, doi:10.1021/es070502d.
- Ervens, B., G. Feingold, G. J. Frost, and S. M. Kreidenweis (2004), A modeling study of aqueous production of dicarboxylic acids: 1. Chemical pathways and speciated organic mass production, *J. Geophys. Res.*, *109*, D15205, doi:10.1029/2003JD004387.
- Fickert, S., J. W. Adams, and J. N. Crowley (1999) Activation of Br₂ and BrCl via uptake of HOBr onto aqueous salt solutions, *J. Geophys. Res.*, *104*(D19), 23,719–23,727, doi:10.1029/1999JD900359.
- Foster, K. L., R. A. Plastridge, J. W. Bottenheim, P. B. Shepson, B. J. Finlayson-Pitts, and C. W. Spicer (2001), The role of Br₂ and BrCl in surface ozone destruction at polar sunrise, *Science*, *291*(5503), 471–474, doi:10.1126/science.291.5503.471.
- Fu, T.-M., D. J. Jacob, F. Wittrock, J. P. Burrows, M. Vrekoussis, and D. K. Henze (2008), Global budgets of atmospheric glyoxal and methylglyoxal, and implications for formation of secondary organic aerosols, *J. Geophys. Res.*, *113*, D15303, doi:10.1029/2007JD009505.
- Giles, K. A., S. W. Laxon, and A. L. Ridout (2008), Circumpolar thinning of Arctic sea ice following the 2007 record ice extent minimum, *Geophys. Res. Lett.*, *35*, L22502, doi:10.1029/2008GL035710.
- Grosjean, D., E. Grosjean, and L. F. R. Moreira (2002), Speciated ambient carbonyls in Rio de Janeiro, Brazil, *Environ. Sci. Technol.*, *36*(7), 1389–1395, doi:10.1021/es0111232.
- Haas, C., A. Pfaffling, S. Hendricks, L. Rabenstein, J.-L. Etienne, and I. Rigor (2008), Reduced ice thickness in Arctic Transpolar Drift favors rapid ice retreat, *Geophys. Res. Lett.*, *35*, L17501, doi:10.1029/2008GL034457.
- Houdier, S., S. Perrier, E. Defrancq, and M. Legrand (2000), A new fluorescent probe for sensitive detection of carbonyl compounds: Sensitivity improvement and application to environmental water samples, *Anal. Chim. Acta*, *412*(1–2), 221–233, doi:10.1016/S0003-2670(99)00875-2.
- Houdier, S., M. Barret, F. Domine, T. Charbouillot, L. Deguillaume, and D. Voisin (2011), Sensitive determination of glyoxal, methylglyoxal and hydroxyacetaldehyde in environmental water samples by using Dansylacetamidoxyamine derivatization and liquid chromatography/fluorescence, *Anal. Chim. Acta*, *704*(1–2), 162–173, doi:10.1016/j.aca.2011.08.002.
- Huisman, A. J., J. R. Hottle, K. L. Coens, J. P. DiGangi, M. M. Galloway, A. Kammrath, and F. N. Keutsch (2008), Laser-induced phosphorescence for the in situ detection of glyoxal at part per trillion mixing ratios, *Anal. Chem.*, *80*(15), 5884–5891, doi:10.1021/ac800407b.
- Intrieri, J. M., and M. D. Shupe (2004), Characteristics and radiative effects of diamond dust over the Western Arctic Ocean Region, *J. Clim.*, *17*, 2953–2960, doi:10.1175/1520-0442(2004)017<2953:CAREOD>2.0.CO;2.
- Ip, H. S. S., X. H. H. Huang, and J. Z. Yu (2009), Effective Henry's law constants of glyoxal, glyoxylic acid, and glycolic acid, *Geophys. Res. Lett.*, *36*, L01802, doi:10.1029/2008GL036212.
- Jones, A. E., P. S. Anderson, E. W. Wolff, J. Turner, A. M. Rankin, and S. R. Colwell (2006), A role for newly forming sea ice in springtime polar tropospheric ozone loss? Observational evidence from Halley Station, Antarctica, *J. Geophys. Res.*, *111*, D08306, doi:10.1029/2005JD006566.
- Jouzel, J., and L. Merlivat (1984), Deuterium and oxygen 18 in precipitation: Modeling of the isotopic effects during snow formation, *J. Geophys. Res.*, *89*(D7), 11,749–11,757, doi:10.1029/JD089iD07p11749.
- Kaleschke, L., et al. (2004), Frost flowers on sea ice as a source of sea salt and their influence on tropospheric halogen chemistry, *Geophys. Res. Lett.*, *31*, L16114, doi:10.1029/2004GL020655.
- Kalnajs, L. E., and L. M. Avallone (2006), Frost flower influence on springtime boundary-layer ozone depletion events and atmospheric bromine levels, *Geophys. Res. Lett.*, *33*, L10810, doi:10.1029/2006GL025809.
- Kawamura, K., S. Steinberg, and I. R. Kaplan (1996), Concentrations of monocarboxylic and dicarboxylic acids and aldehydes in southern California wet precipitations: Comparison of urban and nonurban samples and compositional changes during scavenging, *Atmos. Environ.*, *30*(7), 1035–1052, doi:10.1016/1352-2310(95)00404-1.
- Kieber, D. J., and K. Mopper (1987), Photochemical formation of glyoxylic and pyruvic acids in seawater, *Mar. Chem.*, *21*(2), 135–149, doi:10.1016/0304-4203(87)90034-X.
- Knietsch, A., T. Waschkwitz, S. Bowien, A. Henne, and R. Daniel (2003), Metagenomes of complex microbial consortia derived from different soils as sources for novel genes conferring formation of carbonyls from short-chain polyols on *Escherichia coli*, *J. Mol. Microbiol. Biotechnol.*, *5*(1), 46–56, doi:10.1159/000068724.
- Kwok, R., and D. A. Rothrock (2009), Decline in Arctic sea ice thickness from submarine and ICESat records: 1958–2008, *Geophys. Res. Lett.*, *36*, L15501, doi:10.1029/2009GL039035.
- Lacorte, S., J. Quintana, R. Tauler, F. Ventura, A. Tovar-Sanchez, and C. M. Duarte (2009), Ultra-trace determination of persistent organic pollutants in Arctic ice using stir bar sorptive extraction and gas chromatography coupled to mass spectrometry, *J. Chromatogr. A*, *1216*, 8581–8589, doi:10.1016/j.chroma.2009.10.029.
- Lindberg, S. E., S. Brooks, C.-J. Lin, K. J. Scott, M. S. Landis, R. K. Stevens, M. Goodsite, and A. Richter (2002), Dynamic oxidation of gaseous mercury in the Arctic troposphere at Polar sunrise, *Environ. Sci. Technol.*, *36*, 1245–1256, doi:10.1021/es0111941.
- Martin, S., Y. Yu, and R. Drucker (1996), The temperature dependence of frost flower growth on laboratory sea ice and the effect of the flowers on infrared observations of the surface, *J. Geophys. Res.*, *101*(C5), 12,111–12,125, doi:10.1029/96JC00208.
- Maslanik, J. A., C. Fowler, J. Stroeve, S. Drobot, J. Zwally, D. Yi, and W. Emery (2007), A younger, thinner Arctic ice cover: Increased potential for rapid, extensive sea-ice loss, *Geophys. Res. Lett.*, *34*, L24501, doi:10.1029/2007GL032043.
- Møller, A. K., T. Barkay, W. A. Al-Soud, S. J. Sørensen, H. Skov, and N. Kroer (2011), Diversity and characterization of mercury-resistant bacteria in snow, freshwater and sea-ice brine from the High Arctic, *FEMS Microbiol. Ecol.*, *75*(3), 390–401, doi:10.1111/j.1574-6941.2010.01016.x.
- Mopper, K., and D. J. Kieber (1991), Distribution and biological turnover of dissolved organic compounds in the water column of the Black Sea, *Deep Sea Res. Part A*, *38*, suppl. 2, S1021–S1047.
- Morin, S., G. M. Marion, R. von Glasow, D. Voisin, J. Bouchez, and J. Savarino (2008), Precipitation of salts in freezing seawater and ozone depletion events: A status report, *Atmos. Chem. Phys.*, *8*, 7317–7324, doi:10.5194/acp-8-7317-2008.
- Mullins, W. W., and R. F. Sekerka (1963), Morphological stability of a particle growing by diffusion or heat flow, *J. Appl. Phys.*, *34*(2), 323–329, doi:10.1063/1.1702607.
- Nghiêm, S. V., Y. Chao, G. Neumann, P. Li, D. K. Perovich, T. Street, and P. Clemente-Colon (2006), Depletion of perennial sea ice in the eastern Arctic Ocean, *Geophys. Res. Lett.*, *33*, L17501, doi:10.1029/2006GL027198.

- Obbard, R., H. K. Roscoe, E. W. Wolff, and H. M. Atkinson (2009), Frost flower surface area and chemistry as a function of salinity and temperature, *J. Geophys. Res.*, *114*, D20305, doi:10.1029/2009JD012481.
- Perovich, D. K., and J. A. Richter-Menge (1994), Surface characteristics of lead ice, *J. Geophys. Res.*, *99*(C8), 16,341–16,350, doi:10.1029/94JC01194.
- Perri, M. J., S. Seitzinger, and B. J. Turpin (2009), Secondary organic aerosol production from aqueous photooxidation of glycolaldehyde: Laboratory experiments, *Atmos. Environ.*, *43*(8), 1487–1497, doi:10.1016/j.atmosenv.2008.11.037.
- Pučko, M., G. A. Stern, D. G. Barber, R. W. Macdonald, and B. Rosenberg (2010a), The International Polar Year (IPY) Circumpolar Flaw Lead (CFL) System Study: The importance of brine processes for α - and γ -hexachlorocyclohexane (HCH) accumulation or rejection in sea ice, *Atmos. Ocean*, *48*, 244–262, doi:10.3137/OC318.2010.
- Pučko, M., G. A. Stern, R. W. MacDonald, D. G. Barber (2010b), α - and γ -hexachlorocyclohexane measurements in the brine fraction of sea ice in the Canadian High Arctic using a sump-hole technique, *Environ. Sci. Technol.*, *44*, 9258–9264, doi:10.1021/es102275b.
- Quinby-Hunt, M. S., and K. K. Turekian (1983), Distribution of elements in sea water, *Eos Trans. AGU*, *64*(14), 130–132, doi:10.1029/E0064i014p00130.
- Rankin, A. M., E. W. Wolff, and S. Martin (2002), Frost flowers: Implications for tropospheric chemistry and ice core interpretation, *J. Geophys. Res.*, *107*(D23), 4683, doi:10.1029/2002JD002492.
- Richter, A., F. Wittrock, M. Eisinger, and J. P. Burrows (1998), GOME observations of tropospheric BrO in Northern Hemisphere spring and summer 1997, *Geophys. Res. Lett.*, *25*(14), 2683–2686, doi:10.1029/98GL52016.
- Rigor, I. G., and J. M. Wallace (2004), Variations in the age of Arctic sea ice and summer sea ice extent, *Geophys. Res. Lett.*, *31*, L09401, doi:10.1029/2004GL019492.
- Rothrock, D. A., D. B. Percival, and M. Wensnahan (2008), The decline in arctic sea-ice thickness: Separating the spatial, annual, and interannual variability in a quarter century of submarine data, *J. Geophys. Res.*, *113*, C05003, doi:10.1029/2007JC004252.
- Schroeder, W. H., K. G. Anlauf, L. A. Barrie, J. Y. Lu, A. Steffen, D. R. Schneeberger, and T. Berg (1998), Arctic springtime depletion of mercury, *Nature*, *394*, 331–332, doi:10.1038/28530.
- Serreze, M. C., M. M. Holland, and J. Stroeve (2007), Perspectives on the Arctic's shrinking sea-ice cover, *Science*, *315*, 1533–1536, doi:10.1126/science.1139426.
- Shaw, S. L., B. Gantt, and N. Meskhidze (2010), Production and emissions of marine isoprene and monoterpenes: A review, *Adv. Meteorol.*, *2010*, 408696, doi:10.1155/2010/408696.
- Shepson, P. B., P. Matrai, L. Barrie, and J. W. Bottenheim (2003), Ocean-atmosphere-sea ice-snowpack interactions in the Arctic, and global change, *Eos Trans. AGU*, *84*(36), 349, 355, doi:10.1029/2003EO360002.
- Sherman, L. S., J. D. Blum, T. A. Douglas, and A. Steffen (2012), Frost flowers growing in the Arctic ocean–atmosphere–sea ice–snow interface: 2. Mercury exchange between the atmosphere, snow and frost flowers, *J. Geophys. Res.*, *117*, D00R10, doi:10.1029/2011JD016186.
- Sigsby, J. E., S. Tejada, W. Ray, J. M. Lang, and J. W. Duncan (1987), Volatile organic compound emissions from 46 in-use passenger cars, *Environ. Sci. Technol.*, *21*(5), 466–475, doi:10.1021/es00159a007.
- Simpson, W., L. D. Carlson, G. Honninger, T. A. Douglas, M. Sturm, D. Perovich, and U. Platt (2007a), First-year sea ice contact predicts bromine monoxide (BrO) levels at Barrow, Alaska better than potential frost flower contact, *Atmos. Chem. Phys.*, *7*, 621–627, doi:10.5194/acp-7-621-2007.
- Simpson, W., et al. (2007b), Halogens and their role in polar boundary-layer ozone depletion, *Atmos. Chem. Phys. Discuss.*, *7*(2), 4285–4403, doi:10.5194/acpd-7-4285-2007.
- Sinreich, R., S. Coburn, B. Dix, and R. Volkamer (2010), Ship-based detection of glyoxal over the remote tropical Pacific Ocean, *Atmos. Chem. Phys.*, *10*(23), 11,359–11,371, doi:10.5194/acp-10-11359-2010.
- Stavrakou, T., J. F. Müller, I. De Smedt, M. Van Roozendael, M. Kanakidou, M. Vrekoussis, F. Wittrock, A. Richter, and J. P. Burrows (2009), The continental source of glyoxal estimated by the synergistic use of spaceborne measurements and inverse modelling, *Atmos. Chem. Phys.*, *9*(21), 8431–8446, doi:10.5194/acp-9-8431-2009.
- Steffen, A., et al. (2007), A synthesis of atmospheric mercury depletion event chemistry linking atmosphere, snow and water, *Atmos. Chem. Phys. Discuss.*, *7*, 10,837–10,931, doi:10.5194/acpd-7-10837-2007.
- Stroeve, J., M. M. Holland, W. Meier, T. Scambos, and M. Serreze (2007), Arctic sea ice decline: Faster than forecast, *Geophys. Res. Lett.*, *34*, L09501, doi:10.1029/2007GL029703.
- Stumm, W., and J. J. Morgan (1996), *Aquatic Chemistry: Chemical Equilibria and Rates in Natural Waters*, 3rd ed., 1040 pp., Wiley-Intersci., Hoboken, N. J.
- Style, R. W., and M. G. Worster (2009), Frost flower formation on sea ice and lake ice, *Geophys. Res. Lett.*, *36*, L11501, doi:10.1029/2009GL037304.
- Volkamer, R. (2005), DOAS measurement of glyoxal as an indicator for fast VOC chemistry in urban air, *Geophys. Res. Lett.*, *32*, L08806, doi:10.1029/2005GL022616.
- Wolff, E. W., A. M. Rankin, and R. Röthlisberger (2003), An ice core indicator of Antarctic sea ice production?, *Geophys. Res. Lett.*, *30*(22), 2158, doi:10.1029/2003GL018454.
- Zeng, T., Y. Wang, K. Chance, E. V. Browell, B. A. Ridley, and E. L. Atlas (2003), Widespread persistent near-surface ozone depletion at northern high latitudes in spring, *Geophys. Res. Lett.*, *30*(24), 2298, doi:10.1029/2003GL018587.
- Zhou, X., and K. Mopper (1990), Apparent partition coefficients of 15 carbonyl compounds between air and seawater and between air and freshwater; implications for air-sea exchange, *Environ. Sci. Technol.*, *24*(12), 1864–1869, doi:10.1021/es00082a013.
- Zhou, X., and K. Mopper (1997), Photochemical production of low-molecular-weight carbonyl compounds in seawater and surface microlayer and their air-sea exchange, *Mar. Chem.*, *56*(3–4), 201–213, doi:10.1016/S0304-4203(96)00076-X.
- C. Anastasio and H. J. Beine, Department of Land, Air, and Water Resources, University of California, One Shields Ave., Davis, CA 95616, USA. (canastasio@ucdavis.edu; hbeine@ucdavis.edu)
- M. Barret, F. Domine, and S. Houdier, Laboratoire de Glaciologie et Géophysique de l'Environnement, Université Joseph Fourier-Grenoble I, BP 96, F-38402 Saint-Martin d'Hères CEDEX, France. (barret@lgge.obs.ujf-grenoble.fr; florent@lgge.obs.ujf-grenoble.fr; stephan@lgge.obs.ujf-grenoble.fr)
- J. Bottenheim, S. Netcheva, R. Staebler, and A. Steffen, Air Quality Research Division, Environment Canada, 4905 Dufferin St., Toronto, ON M3H 5T4, Canada. (jwbottenheim@gmail.com; stoyka.netcheva@ec.gc.ca; ralf.staebler@ec.gc.ca; alexandra.steffen@ec.gc.ca)
- T. A. Douglas, U.S. Army Cold Regions Research and Engineering Laboratory, PO Box 35170, Fort Wainwright, AK 99703, USA. (thomas.a.douglas@usace.army.mil)
- A. Grannas and G. Rowland, Department of Chemistry, Villanova University, 800 Lancaster Ave., Villanova, PA 19085, USA. (amanda.grannas@villanova.edu; glenn.rowland@villanova.edu)